ELSEVIER

Biophysical Chemistry 60 (1996) 1–16

Biophysical Chemistry

Ionic conductivity, transference numbers, composition and mobility of ions in cross-linked lysozyme crystals

T.Ya. Morozova [1], G.S. Kachalova, N.F. Lanina, V.U. Evtodienko, A.S. Botin, E.A. Shlyapnikova, V.N. Morozov [*,2]

Institute of Theoretical and Experimental Biophysics of the Russian Academy of Sciences, 142292 Pushchino, Moscow region, Russia

Received 2 May 1995; revised 15 December 1995; accepted 18 December 1995

Abstract

Micromethods for measurements of electric conductivity, transference numbers and concentrations of inorganic ions within immobilized protein crystals have been developed and applied to study tetragonal lysozyme crystals cross-linked with glutaraldehyde. Donnan equilibria and mobilities of ions in this crystal were calculated using the data of these methods and the data of crystal pH titration. Taken together these results characterize the lysozyme crystal as an ion exchanger whose electrical properties and ion composition differ greatly from those of the external solution. Although anions transfer most of the current in the crystals, anion mobility is considerably lower than that of cations. Mobility of all ions in the crystal is considerably lower than in solution (3.5–50 times for cations and 120–330 times for anions) and depends on steric restrictions and charges of both ions and lysozyme molecules. Similar features in behavior of crystalline and biological channels are discussed.

Keywords: Ionic composition; Electric conductance; Transference numbers; Ionic mobility; pH titration curve; Lysozyme crystals

1. Introduction

Studies of the transport of solvent, solute molecules and ions in protein monocrystals are interesting from several points of view. First, the transport parameters are important in studying the ability of protein molecules to bind ligands and to catalyze reactions within the crystals. On one hand, these procedures are widely used to check whether the properties of proteins are the same in crystals and in solutions [1]. On the other hand, immobilized enzyme crystals have been recently shown to be a promising material for making chemosensitive elements of biosensors [2,3] and highly stable catalysts for biotechnological purposes [4]. Such applications based on the interactions of specific substances with protein molecules within a crystalline lattice also require an in depth analysis of mechanisms which determine solution composition and transport of in-

* Corresponding author.

[1] Present address: New York University, Department of Chemistry, 31 Washington Place, Room 1018, Box 5, New York, NY 10003, USA. Tel.: (212)998-8755; fax: (212)260-7905; e-mail: morozov@is2.nyu.edu.

[2] Present address: New York University, Department of Chemistry, 31 Washington Place, Room 1018, Box 5, New York, NY 10003, USA. Tel.: (212)998-8755; fax: (212)260-7905; e-mail: morozov@is2.nyu.edu.

0301-4622/96/$15.00 © 1996 Elsevier Science B.V. All rights reserved
PII S0301-4622(96)00007-5

organic ions and charged substrate or inhibitor molecules in channels with a cross-section size comparable to the size of these molecules.

Second, protein crystals can be considered as an appropriate model for porous materials with precisely calibrated pores, in which the pore structures as well as some structural features of the water in the pores are known from X-ray analysis with atomic resolution. Pore sizes in protein crystals vary between 0.5 and 5.0 nm and pores occupy 25–70% of the crystal volume [5]. Since about 70% of all the protein surface in protein crystals is exposed to water [6], one can easily estimate, that the porosity of a typical protein crystal, $(1-3) \cdot 10^6$ m^2 kg^{-1}, is comparable to that of the best known porous materials like silica gels and activated carbons. Analysis of transport of water and solute molecules in channels of protein crystals offers a new approach in studies of physical properties of hydrated water near a protein surface [7]. It may also help to understand physical mechanisms underlying the function of channels in living cells, and processes in membranes for ultrafiltration and reverse osmosis.

The dimensions of protein crystals (not exceeding 0.3–0.5 mm in most cases) are too small for routine methods of electrical measurements. The aim of the present study was to elaborate adequate methods for measurements of concentrations of inorganic ions and ion mobility-related parameters of small crystalline protein samples and to analyze factors which the measured parameters depend on.

2. Materials and methods

2.1. Tetragonal crystals of hen egg-white lysozyme

Tetragonal crystals of hen egg-white lysozyme ($P4_32_12$) were grown according to a slightly modified method of Steinrauf [8] and cross-linked as described in our previous paper [9]. Membranous samples were made of cross-linked crystals (0.5–1 mm in size) by cutting slices parallel to the (001) plane of the crystal with a microtome. Thickness of the microtome sections, controlled by means of a Linnik's microinterferometer as described in [9], was 7–10 μm.

2.2. Measurements of the ionic conductivity of crystals and solutions

Two methods were used to measure the ionic conductivity of crystals. In the first one a microtome section of the crystals was attached with a cyanoacrylate glue to the end of a platinum electrode sealed in a glass tube, as presented schematically in Fig. 1A. The glassy cover of the electrode was treated with 3-aminopropyltriethoxysilane [10] and then with 5% glutaraldehyde in 10 mM phosphate buffer (pH 7.0) to increase its adhesive ability. The

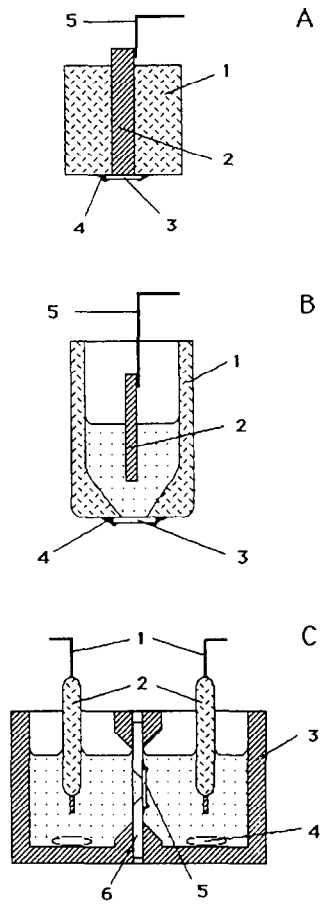

Fig. 1. Schematic of the methods used to measure the specific conductance (A and B) and transference number of ions in protein crystals (C). A and B: 1 = glass capillary, 2 = Pt electrode, 3 = microtome cross-section of the protein crystal, 4 = glue and 5 = connecting wire. C: 1 = connecting wires, 2 = calomel electrodes, 3 = double-chamber cell, 4 = stir bars, 5 = protein sample and 6 = glass plate with a small hole.

diameter of the working surface of the platinum electrode was 100–250 μm. To decrease the surface impedance of the electrode, it was electrochemically covered with platinum black in Kohlrausch's solution as described in Ref. [11]. The crystalline plates were glued to the electrodes in a humid chamber at a humidity of 95–100% to avoid drying and shrinkage of the protein samples. To prevent formation of a gas layer and bubbles between the electrode and the sample, the gap was filled with a gel-forming protein solution. A small droplet of a freshly prepared mixture of 10% serum albumin and 2.5% glutaraldehyde in 50 mM phosphate buffer was placed on the electrode, covered with sample and immediately pressed to the surface. Most of the mixture was squeezed out to bring the sample into direct contact with the electrode surface. The sample edges protruding the platinum electrode boundaries were then glued to the glass cover with the cyanoacrylate glue. After polymerization of the cyanoacrylate the electrodes with the samples were stored in the salt buffer solution used in the lysozyme crystallization (5% NaCl, 50 mM sodium acetate buffer, pH 4.7).

Measurements of the conductivity of lysozyme crystals were performed in a thermostated cell with three platinum electrodes, of which only one had sample glued to it. One of the free electrodes was connected to the measuring AC bridge (TESLA, BM 401 or R568), the two others were connected by turns. The sample resistance was calculated as a difference of resistances, $R_{cr} = R_c - R_s$, between two pairs of electrodes, one of which contained the sample, R_c, and the second the two free electrodes, R_s. To exclude the contribution of the electrodes impedance we plotted R_c and R_s values as functions of the inverse square root of frequency, $(\nu^{-1/2})$, and extrapolated them to the infinite frequency as described in [11]. The measurements were made in the frequency range of 1.5–10 kHz; the amplitude of the AC voltage on the sample never exceeded 25 mV.

Crystal conductivity κ_{cr}, was calculated according to the expression:

$$\kappa_{cr} = h/\pi r^2 R_{cr} \quad (1)$$

Here r and h are the radius of the platinum electrode and the thickness of the sample. The expression 1 is valid for $h \ll r$. Using the known formula for the resistance of a pair of small distant disc shaped electrodes in solution [12], $R_s = 1/2r\kappa_s$, the ratio between solution and crystal conductivity can be found from the formula:

$$\kappa_s/\kappa_{cr} = \pi r R_{cr}/2hR_s \quad (2)$$

In another method of measurement of crystal conductivity, schematically presented in Fig. 1B, protein sample covered a conical hole at the end of a glass capillary filled with buffer solution. One platinum electrode was placed inside the capillary, another in the external buffer solution. The large surface of the electrodes used in this method obviated the necessity to account for their impedance, making it possible to use an automatic bridge working at a fixed frequency (1 or 10 kHz, R5016 bridge). Sample resistance was calculated as a difference in the resistances of the capillary with and without sample, when it was filled with the same buffer. The crystal conductivity was then calculated according to Eq. (1).

Both methods gave comparable results with protein samples measured under identical conditions. This is indicative of the negligible effects of the thin and far more conductive albumin gel spacer (with a conductivity close to that of solution) on the measured conductivity of protein crystals in the first method. The errors in measurements of κ_s/κ_{cr} did not exceed 5%. This value mainly arises from the precision of the microinterferometric measurements of sample thickness.

Conductance of buffer solutions was measured at 18°C using a commercial conductance meter, YSI, Model 35, and a thermostated vessel. The conductivity vessel constant was measured with standard KCl solutions [13] and absolute values of the conductivity of solutions were calculated. Measurements with independently prepared solutions showed the same conductivity within a 2% precision.

2.3. Activation energy of crystal conductance

Control experiments have shown that the temperature dependence of the logarithm of conductance of the lysozyme crystals is a linear function of T^{-1} in the range between room temperature and 55°C. This allows to characterize temperature dependence in terms of effective activation energy. Routinely, the activation energy of crystal conductance was mea-

sured between 16 and 26°C. The dispersion of the values measured under identical conditions was ±1 kJ/mol.

2.4. Measurement of ionic transference numbers

In this method the crystalline plate covered a conical hole in a thin (0.14–0.17 mm) glass cover slip, which divided two 2-ml cells filled with salt solutions, as shown in Fig. 1C. The hole with the input diameter of 0.1 mm and the output one of 0.4 mm was drilled with a tungsten wire and a diamond powder. Before gluing sample to the smaller outlet of the conical hole, the glass cover slip was treated with 3-aminopropyltriethoxysilane, as described above. The measuring cell was not thermostated, but in each experiment temperature of the solutions was registered and the temperature change during experiments never exceeded 1°C.

The difference in the transference numbers of anions and cations, Δt, was calculated from the diffusion potential, $\Delta\phi_d$, measured between the two cells filled with different salt solutions. If C_1 and C_2 are the concentrations of the salt solutions, then, according to a simple thermodynamic relation [14]:

$$t^- - t^+ = \Delta t = F\Delta\phi_d / [RT \ln(C_1/C_2)] \quad (3)$$

Here F and R are the Faraday and gas constants, T is the absolute temperature. $\Delta\phi_d$ was measured with a digital voltmeter connected to the solutions via a pair of calomel electrodes providing a stability in the potential measurements of about 0.1–0.2 mV in 10 min. C_1 and C_2 in experiments at low salt concentration were chosen to be 0.05 M and 0.1 M, and they were 0.8 M and 1.0 M in experiments at high salt concentrations. Since control experiments did not reveal any dependence of $\Delta\phi_d$ on the rate of stirring of the solution, we conclude that the diffusion potential originates within the protein membrane.

The largest errors in measurements of the transference numbers were observed at low pH (pH 4.0) and low salt concentrations. In a series of 5 independent measurements in these conditions r.m.s. deviation in the t^-/t^+ value did not exceed 20%.

Measurements of both conductivity and of transference numbers were performed under constant stirring of the solutions.

2.5. Intracrystalline concentration of Br^- ions

The intracrystalline concentration of Br^- ions was determined by the intensity of X-ray fluorescence of the ions. A thin-walled quartz capillary 1.5 mm in diameter with glass wool in its lower end (to keep crystals immobile in the solution flow) was filled with cross-linked protein crystals and attached to a goniometer head in a measuring device. A continuous flow of solution with a rate of about 10 ml/h made rapid changes possible in the composition of the buffer surrounding crystals. Measurements were made at room temperature (18–22°C).

To excite X-ray fluorescence a DRON X-ray source equipped with a BSV-27 tube (copper anode) working under 15 kV and 4 mA was used. The diameter of the collimated beam was 0.5 mm. Fluorescence intensity was measured with the ORTEC Si(Li) semiconductor X-ray detector equipped with a multichannel energy analyzer. The analyzer was calibrated using the ^{55}Fe isotope. Fluorescence spectra were accumulated for 40 s. The integral intensity of the ion fluorescence was corrected by subtracting the intensity of the background, which was measured in the same energy interval in the absence of ions in solution.

The intracrystalline concentration of the Br^- was determined from a calibration curve obtained for every capillary by filling it with solutions of NaBr at known concentrations. After correction for the background, the fluorescence intensity of Br was found to be a linear function of the Br^- concentration within 20–300 mM both in the absence and in the presence of 1 M NaCl in the solution. On increasing the Br^- concentration above 300 mM a deviation from linearity was observed.

When calculating the concentration of Br^- ions in the crystal we took into account that fluorescence of a NaBr solution between the crystals in the capillary also contributes to the measured fluorescence intensity. To determine the volume fraction of the capillary occupied by the solution, α, we used the fluorescence of Rb^+ ions, which were shown not to penetrate notably inside the lysozyme crystals at low pH (4.0) and low salt concentration (0.02 M). Under these conditions fluorescence intensities in the Rb energy range were measured for capillaries filled with (i) buffer, I_b, (ii) 20 mM RbCl in the buffer,

I_{Rb}, (iii) crystals in the buffer, I_{cr}, and (iv) crystals in RbCl solution on the same buffer, I_{crRb}. The solution-filled fraction of the capillary interior was then determined from the relation:

$$\alpha = (I_{crRb} - I_{cr})/(I_{Rb} - I_b) \quad (4)$$

This was found to be 0.5 ± 0.1. All intensities were corrected for the background.

The molar Br^- concentration assigned to the unit of crystal volume, Br_{cr}^-, was determined from the calibration curve, using the corrected intensity of the Br line:

$$I_{corr} = [I_{crBr} - I_{cr} - \alpha(I_{Br} - I_b)]/(1 - \alpha) \quad (5)$$

Here I_{Br} is the fluorescence intensity of the capillary filled with NaBr solution, I_{crBr} is that when the capillary is filled with protein crystals in equilibrium with the NaBr solution. All the salt solutions were prepared in the same buffer, specified below. Due to the large background fluorescence of buffer solution the minimum Br_{cr}^- concentration measurable by this method was 5 mM. X-ray fluorescence applied here for Br analysis, can also be used for the analysis of any element in the protein crystal, provided that its atomic mass > 40. The method will be described in more details elsewhere.

2.6. Potentiometric titration of lysozyme crystals

The potentiometric titration of lysozyme crystals was performed in a 1 M solution of NaCl to minimize the curve shift due to the difference in the external and internal pH, resulting from the Donnan potential. Titration was done under nitrogen using a PHM83 Radiometer (Denmark) pH meter equipped with a TTT80 titrator, an ABV80 autoburette and a titration cell ITA80. Measurements were done at room temperature. Special small immobilized crystals (1–5 μm in size) were prepared for the titration experiment, since large crystals (0.1–0.5 mm) were shown to be titrated extremely slow at neutral pH. The equilibrium in the crystal suspension was considered to be achieved when the rate of pH change was ≤ 0.003 pH units per min. Titration was performed with 0.1 M solutions of NaOH or HCl containing 1 M NaCl. The crystals used in the experiment were preequilibrated in a 1 M NaCl solution for a few days with 3–4 changes of buffer solution. Before titration nitrogen was bubbled through the intensively stirred solutions for about 30 min until a constant pH reading was achieved. After the titration experiment the crystals were thoroughly dialyzed against distilled water and then dried at 135°C up to a constant weight, which was used in calculating the titration curve. The titration curve, $Z(pH_{out})$, was obtained as a result of deduction of the titration curve of the 1 M NaCl solution from that of the crystal suspension. The true titration curve of the crystalline lysozyme, $Z(pH_{in})$, taking into account the difference in external and internal pH, was calculated by an iteration method as described below.

2.7. Calculation of electrostatic potential and equilibrium ionic concentrations in crystal channels

Taking the initial concentrations of all salts and pH of the external solution and assuming that the composition of this solution does not depend upon the presence of protein crystals (volume of solution, continuously flowing through the capillary, is much larger than that of the crystals), we calculated equilibrium concentrations of ions in the external solution, using known dissociation constants and activity coefficients [15,16]. Since the isoionic point of lysozyme is $pI = 11.2$ [17], at all pH values < 11.2 lysozyme molecules are positively charged. That results in formation of an electrostatic potential, ψ, between the external solution and crystal, which causes redistribution of ions. The ratio of internal, a_{in}, and external, a_{out}, equilibrium molal activity for any ion may be written as [18]:

$$(a_{in}/a_{out}) = \exp(-ne\psi/kT) \quad (6)$$

Here n is the charge of ion, e is the charge of electron, k and T are the Boltzman's constant and absolute temperature, respectively.

Denoting this ratio for monovalent anions as $X = \exp(e\psi/kT)$ we have the following relation between external and internal pH:

$$pH_{in} = pH_{out} + \log X \quad (7)$$

Applying the electroneutrality law to the crystal and expressing molal concentrations in the intracrys-

talline solution through those in the external one we get the equation:

$$\begin{aligned} H_{out} + Na_{out}\left(\gamma_{Na}^{out}/\gamma_{Na}^{in}\right) + X\rho_m Z \\ = \left[\left(10^{-14}/H_{out}\right) + Cl_{out}\left(\gamma_{Cl}^{out}/\gamma_{Cl}^{in}\right)\right. \\ + Br_{out}\left(\gamma_{Br}^{out}/\gamma_{Br}^{in}\right) + Ac_{out}\left(\gamma_{Ac}^{out}/\gamma_{Ac}^{in}\right) \\ \left. + B_{out}\left(\gamma_{B}^{out}/\gamma_{B}^{in}\right) + F_{out}\left(\gamma_{F}^{out}/\gamma_{F}^{in}\right)\right] X^2 \\ + 2F_{out}^{*}\left(\gamma_{F^*}^{out}/\gamma_{F^*}^{in}\right) X^3 \end{aligned} \quad (8)$$

Here Ac, B, F and F^* are molal concentrations of monovalent acetate, borate and phosphate anions and of bivalent phosphate ion, respectively. Z is the net charge of lysozyme molecule at given pH, ρ_m is the molal concentration of lysozyme in crystal. γ^{out}/γ^{in} is the ratio of activity coefficients in external and internal solutions for each ion. According to our data [19] tetragonal lysozyme crystals cross-linked with glutaraldehyde contain $h = 0.451$ kg H_2O per kg of dry protein. Taking $M_w = 14.3$ kg for the molar mass of lysozyme we find that in the tetragonal crystal 1 M of lysozyme molecules is dissolved in $M_w \cdot h$ kg of water. Therefore, $\rho_m = 1/h \cdot M_w = 0.155$ m.

To calculate X, pH_{in}, ψ and the molal concentrations of all ions within the crystalline channels we solved the system of Eqs. (6)–(8) by the iteration method starting from ion concentrations in the external solution, their activity coefficients at these concentrations, pH_{out} and Z of lysozyme from the $Z(pH_{in})$ curve at $pH = pH_{out}$. On each next iteration step new activities of ions and a new value of $Z(pH_{in})$ corresponding to the value of pH_{in} obtained in the preceding step were taken. Four to six iterations were usually enough to get self-consistent results. Since calculations were performed for pH values between 3.0 and 9.0, activity coefficients of H^+ and OH^- were assumed to be 1. Those for other ions were taken from published concentration dependencies [15,16].

To compare with the data of the X-ray fluorescence method, we need ion concentrations to be expressed as molar concentrations attributed to unit of crystal volume. Since according to X-ray data 1 M of lysozyme molecules occupies within cross-linked tetragonal crystals $V_M = 17.84$ l, then molar concentration of lysozyme in this crystal is $\rho_M = (1/V_M)$ $= 0.056$ M. To find molar concentrations of ions from the molal concentrations we need to multiply the latter by a coefficient $\alpha = hM_w/V_M = 0.36$.

2.8. Calculations of ion mobilities

Upper estimates for mobility of ions inside the crystal were made by using experimental data on crystal conductivity, κ_{cr}, and experimental transference numbers of ions, t^+ and t^-, and taking equilibrium molar concentrations of ions in crystal, C_{cr}^-, C_{cr}^+, calculated by the method described above:

$$U_{cr}^+ = \kappa_{cr}/\left[1 + (t^-/t^+)\right] F \cdot C_{cr}^+ \quad (9)$$

$$U_{cr}^- = \kappa_{cr}(t^-/t^+)/\left[1 + (t^-/t^+)\right] F \cdot C_{cr}^- \quad (10)$$

Here F is the Faraday's constant. These equations give estimates for the upper level of ion mobility, since they do not take into account, that protein molecules may bind ions specifically. Under such conditions real concentration of ions in crystal must be higher and their average mobility lower. The intracrystalline concentration of some ions may be lower than predicted by Donnan equilibria if their sizes are equal or exceed those of the bottle necks in the crystal channels. However, all the ions, we are dealing with here, have hydrated radii small enough to easily penetrate the crystal (see Fig. 8).

To estimate the mobility of cations, that of Na^+ was first calculated for the crystal in equilibrium with a NaCl solution in the buffer, since Na^+ was the only cation in this solution (except for a negligible concentration of H^+). When calculating U_{cr}^+ of other cations we made a correction for the contribution of additional 15 mM of Na^+ from the buffer in the external solution into the total cation conductivity of the crystal, κ_{cr}^+.

We failed to make the same correction for the contribution of buffer anions into the total anion conductivity of the crystal, κ_{cr}^-, since equivalent conductivities of these anions in the crystal were not measured. Therefore, only upper and lower estimates of U_{cr}^- were obtained. The lower estimate was based on an assumption that all anions have similar mobility and the total concentration of all anions in the crystal was substituted as C_{cr}^- in Eq. (10). In the upper estimate we neglected the contribution from buffer anions at all (only the concentration of salt

anion was substituted into Eq. (10)). As can be seen from Table 3, maximum difference between these two estimates is observed under low salt concentration at pH 9.0, when concentrations of buffer anions and salt anions in the crystal become comparable.

2.9. Measurements of crystal deformation

Measurements of crystal deformation resulting from pH and salt concentration changes were made in the buffer solution in a thermostated cell. An optical microscope equipped with an ocular micrometer was used to measure the deformation of microtome sections of cross-linked lysozyme crystals.

2.10. Buffer composition

To maintain the pH in a broad range a complex buffer was used, consisting of NaAc, Na_2HPO_4 and H_3BO_3, 5 mM each. The pH was adjusted with NaOH and HCl solutions. All chemicals used were of analytical chemical reagent grade.

3. Results

3.1. Measurements of the crystal deformation due to pH and salt concentration changes

Measurements of the crystal deformation due to pH and salt concentration changes were performed in the pH range of 2.0–11.0 and at a NaCl concentration from 0 to 1 M. No noticeable changes in crystal dimensions within 0.1% precision of the measurements were detected in the pH interval of 3.0–9.0. However, a decrease of pH below 3.0 and to a greater extent an increase above 9.0 at low salt concentration (0.02 M) resulted in a shrinkage of the tetragonal crystals along [001] direction and swelling in the (001) plane. X-ray experiments detect progressive fading away of the reflections with higher indices in the reciprocal lattice that is indicative of a distortion of the crystal structure at pH > 9.5. pH-titration experiments also reveal some rearrangements in the tetragonal crystals at pH > 9.2. They proceed so slow that after addition of a small aliquot of NaOH solution pH equilibrium was not reached in a day at this pH, whereas at other pH values 10–40 min was enough to establish the equilibrium in small (1–5 μm) crystals. That is why all the measurements of conductance and transference numbers were done in the pH interval of 4.0–9.0, where size and structure of the crystals are not changed and do not affect electrical properties of the crystals.

The effect of addition of 1 M NaCl to the buffer solution was pH dependent, crystal dimensions decrease along the [001] direction (z axes) by 0.25–1%, and in the (001) plane by no more than 0.25%. These changes do not seem significant. Our computer simulation of the diffusion of an uncharged ball in the tetragonal lysozyme crystal has recently shown, that bottle necks in the channels along [001] direction have sizes of about 11 Å [7]. Even if we assume, that all 1% shrinkage along this direction is due to a decrease in the size of this bottle necks, the channel diameter will decrease only by 0.38 Å (i.e., 1% of the unit cell parameter c = 37.6 Å). According to the above-mentioned simulations, the diffusion coefficient and mobility should decrease by about 30% for an ion with a hydrated radius similar to that of Na^+,

Table 1
Transference number ratios for anions and cations, (t_{cr}^-/t_{cr}^+), measured along the [001] direction in the tetragonal lysozyme crystal at different concentrations of salts [a] and at different pH values in the external solution [b]

C (M)	pH_{out}	LiCl	NaCl	KCl	CsCl	NH_4Cl	KBr	KNO_3
0.075	4.0	15.6	8.5	5.1	4.2	4.4	4.7	3.8
0.075	9.0	4.3	3.8	3.4	3.1	2.0	2.3	2.2
0.9	4.0	2.5	2.3	2.2	2.2	2.1	2.5	1.8
0.9	9.0	1.3	1.3	1.3	1.1	1.2	1.1	1.0

[a] $C = (C_1 + C_2)/2$, where C_1 and C_2 are concentrations of salt in the two chambers, between which the diffusion potential was measured.
[b] Measurements were made at 18°C in the buffer specified in Materials and Methods. Maximum r.m.s. in the t_{cr}^-/t_{cr}^+ ratio was observed at low (0.075 M) salt at pH = 4.0, where it was ±20%.

$r_h = 3.9$ Å. Experimentally measured many-fold decrease in the mobility of Na^+ and increase in the mobility of Cl^- as result of the salt addition (see Table 3) make us believe, that not small crystal deformation but some other factors induce the observed large changes in ion mobility.

3.2. Transference numbers

Transference numbers of different ions measured for different salts at different pH values and salt concentrations are presented in Table 1. The data are in complete agreement with the fact, that lysozyme molecules are positively charged at all pH values < $pI = 11.2$ [17]: motion of anions is responsible for most of the current in the crystal. Transference numbers of cations and anions become comparable only at high (0.9 M) salt concentration at pH 9.0, i.e., when positive charge immobilized on channel walls becomes small ($z = +4.5$) and highly screened. As Table 1 shows, the ratio of the transference numbers depends on the type of salt used. In series of 0.1 M solutions of monovalent chlorides at pH 4.0 a nearly linear inverse dependence of t^+ on the hydrated radius of ions [20] is observed: t^+/r_h for Li^+, Na^+, K^+ and Cs^+ is 0.06/4.51 Å, 0.105/3.9 Å, 0.164/3.36 Å and 0.192/3.07 Å, respectively. Previously, De Villardi et al. [21] have obtained similar data for t^+ of Na^+ and K^+ in amorphous lysozyme films. However, the ionic selectivity of this film was worse than in our crystals (0.160 and 0.162 for Na^+ and K^+), presumably due to larger and less homogeneous channels.

3.3. Ionic conductivity and its activation energy

According to our gravimetric measurements of hydration and X-ray measurements of unit cell parameters of cross-linked lysozyme crystals [19], water (and hence, the channels) occupies 36% of the volume in tetragonal and 25% in triclinic crystals. Assuming a uniform distribution of channels over the crystals, one can estimate that channels occupy 24% and 16.6% of the cross-section in the tetragonal and triclinic crystals, respectively. This would result in a decrease of conductivity of these crystals by a factor of 4 and 6 as compared to the conductivity of solutions. The data presented in Fig. 2 and in Table 2 indicate, that the κ_s/κ_{cr} ratio in the triclinic crystal is larger than in the tetragonal one, as expected. However, at all pH and salt concentrations studied the values of κ_s/κ_{cr} are 10–30 times larger than expected. This suggests, that not the average cross-

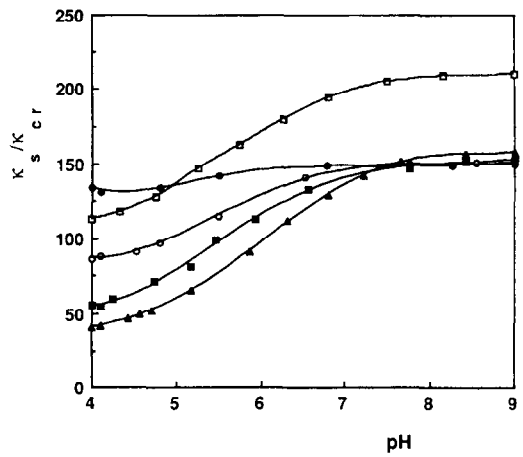

Fig. 2. pH dependence of the ratio of specific conductances of lysozyme crystals, κ_{cr}, and those of solutions, κ_s, in which the crystals were soaked. (□) Triclinic crystal measured at 21°C in 0.1 M NaCl dissolved in the buffer specified in Materials and Methods. All other curves are for the tetragonal lysozyme along the [001] direction. Measurements were done at 19°C in solutions of different NaCl concentrations prepared in the same buffer: (▲) 0.05 M NaCl, (■) 0.1 M NaCl, (○) 0.3 M and (●) 1 M NaCl.

Table 2
Ratio of conductivity of salt solutions [a], κ_s, to that of the crystal (equilibrated with the same salt solution), κ_{cr}, and activation energies of crystal conductivity in different salts and under different pH values

Parameter	pH	LiCl	NaCl	KCl	CsCl	KBr	KNO_3
κ_s/κ_{cr}	4.2	52	57	61	67	78	71
κ_s/κ_{cr}	8.2	125	142	117	150	155	142
E_a (kJ/M)	4.2	19.7	21.8	20.9	22.2	21.4	22.2
E_a (kJ/M)	8.2	17.6	16.7	16.7	20.5	17.6	16.7

[a] Measurements of κ_s/κ_{cr} are performed at 20°C in 0.1 M salt solutions prepared in the buffer specified in Materials and Methods. Standard deviation in the measurements of κ_s/κ_{cr} is ±5%. for the activation energy this is ± 1 kJ/mol.

Table 3
Electrostatic (Donnan) potential, Ψ, conductivity of crystal, κ_{cr}, conductivity of solution, κ_s, concentrations and mobilities, U, of ions in NaCl solutions [a] and in tetragonal lysozyme crystal at 18°C

pH_{out}	pH_{in}	ψ (mV)	$\kappa_s \cdot 10^3$ (S/cm)	$\kappa_{cr} \cdot 10^6$ (S/cm)	$\kappa_{cr}^- \cdot 10^6$ (S/cm)	Na [b]			Cl, ΣA_{cr} [b]			
						Na_{out} (mM)	Na_{cr} (mM)	$U_{cr} \cdot 10^{10}$ (m^2/Vs)	Cl_{out} (mM)	Cl_{cr} (mM)	ΣA_{cr} (mM)	$U_{cr} \cdot 10^{10}$ (m^2/Vs)
4.0	5.2	68.7	8.14	157	140	90	1.7	100	84	548	590	2.45–2.64
9.0	9.6	23.4	8.07	53	42	92	7.3	15.5	75	117	223	1.94–3.70
4.0	4.4	35.0	69.4	534	372	915	119	14.1	909	809	814	4.74–4.77
9.0	9.2	8.8	69.2	461	262	917	229	9.1	900	464	476	5.68–5.82

[a] Measurements of κ_s and κ_{cr} were performed at 0.075 M and 0.9 M NaCl in the buffer, specified in Materials and Methods. Ψ, pH_{in}, concentrations and mobilities of ions were calculated as described in Materials and Methods.
[b] Na_{out}, Cl_{out} are molar concentrations of Na^+ and Cl^- in the external solution. Na_{cr}, Cl_{cr} are molar concentrations of these ions attributed to 1 l of the crystal volume. ΣA_{cr} denotes total concentrations all anions in the crystal.
[c] Two estimates for mobility of intracrystalline Cl^- are presented in the last column: low estimate based on the assumption that all anions in solution have similar mobility, and overestimated value obtained by neglecting of the contribution of buffer anions into κ_{cr}^- (see Materials and Methods for more details).

section of channels but rather the channel size in the bottle necks determines the crystal conductivity. The views presented in Fig. 7 clearly show a highly variable character of the crystal channels, with their sizes changing from 6–8 Å to 30–40 Å lengthwise.

As shown in Fig. 2, κ_s/κ_{cr} displays a weak pH dependence at high ionic strength, but the dependence becomes more stronger at a lower salt concentration in solution. The conductivity of the solution itself is only slightly pH dependent, and all observed changes in κ_s/κ_{cr} are due to those in the crystal conductivity, κ_{cr}, which decreases 2–3 times on pH increase at low salt concentrations as can be seen in Table 3. Since anions mainly contribute to κ_{cr} such a decrease in conductivity with pH increase may be explained by a decrease in the anion contribution. As can be seen in Table 3, the decrease in κ_{cr}^- is not due to a drop in the anion mobility, but to a decrease in anion concentration, resulting from a decrease in positive net charge on the lysozyme with pH increase.

Not only κ_{cr}, but also the activation energy of crystal conductivity is pH dependent, as shown in Table 2 and Fig. 3. Variations of E_a in different salts do not exceed the experimental precision, but for all the salts tested E_a increases by 2–5 kJ/mol with pH decrease. Since the increase in E_a occurs together with a decrease in mobility of anions at low pH and salt concentrations, we may suggest, that immobile positive charges on channel walls hinder motion of

Table 4
Conductivity of solutions, κ_s, total conductivity of the tetragonal crystal, κ_{cr}, contribution of cations into this conductivity, κ_{cr}^+, and that of anions, κ_{cr}^-, mobility ratio [a] for ions in solution of different salts [b] to those in crystal, (U_s^+/U_{cr}^+, U_s^-/U_{cr}^-), at pH 4.0 and 18°C

Salt	$\kappa_s \cdot 10^5$ (S/cm)	$\kappa_{cr} \cdot 10^6$ (S/cm)	$\kappa_{cr}^+ \cdot 10^6$ (S/cm)	$\kappa_{cr}^- \cdot 10^6$ (S/cm)	U_s^-/U_{cr}^+	U_s^-/U_{cr}^-
LiCl	746	157	9.5	148	7	240
NaCl	814	156	16.5	140	4.5	260
KCl	958	173	28	145	3.6	250
CsCl	976	159	30.5	128	3.5	280
KBr	965	136	24	112	4.3	330
KNO_3	922	142	30	113	3.4	300

[a] Ion mobilities in solutions were calculated from published data on limiting equivalent ionic conductivity [13]. The upper estimates of U_{cr}^- were taken in calculations of U_s^-/U_{cr}^-. More details concerning calculations of U_{cr}^+ and U_{cr}^- are presented in Materials and Methods.
[b] Measurements were performed in 0.075 M salt solutions prepared on the buffer, specified in Materials and Methods, pH 4.0.

anions. On screening these charges at high salt concentration the pH dependence of E_a gradually disappears and contributions of cations and anions into κ_{cr} become comparable, as can be seen in Fig. 3 and Table 3.

The data in Table 2 indicate significant dependence of κ_s/κ_{cr} on the type of salt. Comparison of the total conductivities of crystals soaked in different chlorides, κ_{cr}, and cation contributions to this conductivity, κ_{cr}^+, (see Table 4) leads to different conclusions about cation selectivity of the channels in lysozyme crystals. Since total crystal conductivity in LiCl, NaCl and CsCl is practically the same, one may erroneously conclude, that channels in the lysozyme crystals are not selective with respect to cations. However, comparison of κ_{cr}^+ shows, that these channels have a cation selectivity sequence similar to that in solution, with larger mobility for cations having smaller hydrated radii. In crystal the selectivity ratio is even larger than in solution: the ratio of κ_{cr}^+ between the largest and the smallest cations in this series, Li^+ to Cs^+, is 3.2 in the crystal and 2 in solution. A similar situation with selectivities was also found in biological channels (like that of acetylcholine receptors), where conductance ratios of different salts and permeability ratios of different cations can yield different selectivity sequences, as it has been shown in [22].

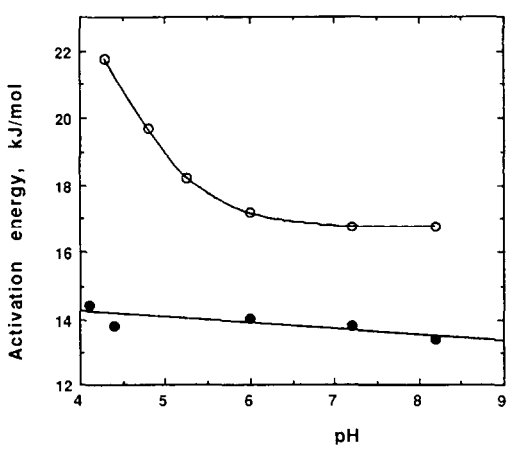

Fig. 3. pH dependence of the activation energy of conductance of the tetragonal lysozyme crystal in [001] direction. Measurements in 1 M NaCl prepared on the buffer specified in Materials and Methods are denoted by (●), those made in the same buffer with 0.1 M NaCl are denoted by (○).

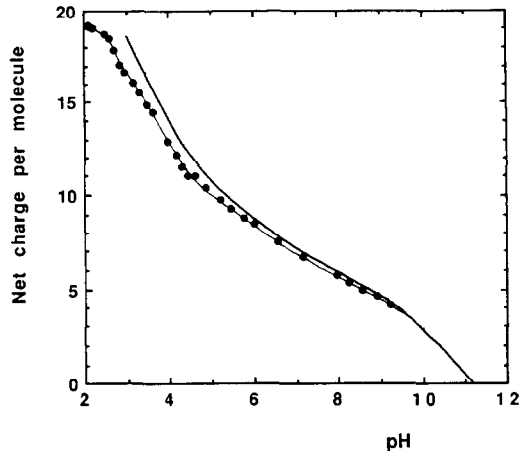

Fig. 4. pH-titration curve of lysozyme in the tetragonal cross-linked crystals. (●) Experimental results of titration in 1 M NaCl further referred to as $Z(pH_{out})$. The solid curve presents the "true" titration curve of crystalline lysozyme, $Z(pH_{in})$, taking into account the pH shift between the external solution and the crystalline channels, as described in Materials and Methods.

Comparison of the data on anion conductivities of different potassium salts, κ_{cr}^-, presented in Table 4, shows, that the size-related sequence does not work for anions in the crystal: Br^- with a hydrated radius smaller than that of Cl^- and NO_3^- [20] has an anomalously small contribution to the crystal conductivity. As we will discuss below, X-ray fluorescence measurements of the intracrystalline Br^- concentration give a proof for a selective binding of Br^-, which might explain their lower mobility and conductivity as compared to Cl^-.

3.4. pH titration, electrostatic potential, calculated and experimental ion concentrations in crystalline channels

This part of our results will be published in detail elsewhere. Here the data are presented to an extent necessary for discussing the electric properties of lysozyme crystals. Fig. 4 gives the pH titration curve of tetragonal lysozyme crystals soaked in 1 M NaCl, $Z(pH_{out})$. The lack of experimental points at pH > 9.2 is explained above (see Section 3.1). Titration was performed in 1 M NaCl to reduce the electrostatic potential and its effect on the intracrystalline pH. Fig. 4 also displays the "true" titration curve of

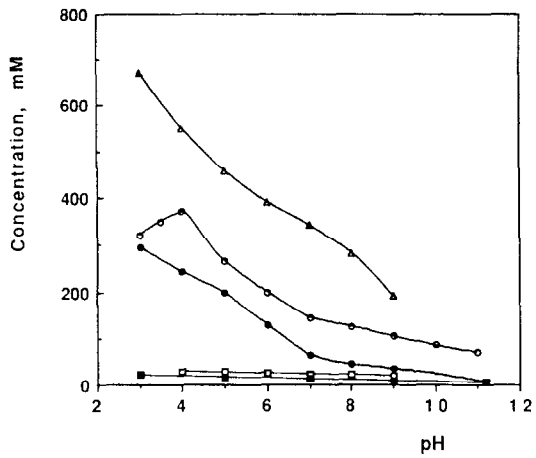

Fig. 5. pH dependence of anion concentrations in the tetragonal lysozyme crystal. (△) The total concentration of anions calculated from the electrostatic potential; (○) experimentally (X-ray fluorescence) measured Br^- concentration; (●) concentration of Br^- calculated from the electrostatic potential; (□ and ■) are the experimental and theoretical Br^- concentrations in the presence of 1 M NaCl. All the above experiments and calculations are made for 20 mM NaBr solution in the buffer, specified in Materials and Methods. Concentrations attributed to 1 l of crystal are presented. These should be divided by $\alpha = 0.36$ (see Materials and Methods) to obtain molal concentrations in crystal channels.

crystalline lysozyme, $Z(pH_{in})$, calculated from the $Z(pH_{out})$ curve as described in Materials and Methods. This "true" curve was then used to calculate ψ and intracrystalline ion concentrations. Results of such calculations are partly presented in Table 3. To test the reliability of our calculations we compared theoretically obtained concentrations with those experimentally determined. Direct analysis of the elemental composition of tetragonal lysozyme crystals, grown in 0.2 M NaAc buffer, pH 4.5, containing 0.855 M NaCl has been made by Palmer et al. [23], and gave 0.5% Na and 3.15% Cl attributed to the dry weight of the crystals. Converted to the molar volume of the hydrated crystals this gives 0.19 M Na and 0.78 M Cl, in excellent agreement with the result of our calculations, which yield under identical conditions 0.18 M Na^+ and 0.79 M Cl^-. This agreement indicates, that for small ions capable of penetrating into the crystal channels electrostatic (Donnan) potential controls the equilibrium internal concentration of ions in just the same way as in polyelectrolyte gels [24,25]. The situation is different for the ions capable of specific binding. Fig. 5 shows the pH dependence of the experimental and calculated molar concentrations of Br^- in the tetragonal crystals with and without 1 M NaCl in solution. It can be seen, that the experimental Br^- concentration in the crystal is much higher than in the surrounding solution at all pH values and salt concentrations (50 times at pH 4.0 and low salt concentration), and always higher than the theoretical ones. Provided it is only potential controlled, we would expect at $pH = pI$, where $\psi = 0$, that the molal Br^- concentration in crystalline channels should be the same as in solution, 0.020 m, or 7.2 mM in molar concentration. Instead, as seen from Fig. 5, the experimental concentration of Br^- never drops to the theoretically expected value. A nearly constant discrepancy of about 70 mM is observed at all pH values except for pH 4.0 and its vicinity, where the experiment shows a maximum corresponding to the additionally binding of about 55 mM of Br^-. Taking into account the molar concentration of lysozyme in the crystal, 56 mM, we may interpret the discrepancy as a result of additional binding of Br^- to two sites on the lysozyme molecule of which one is pH independent and the other has a maximum at pH 4.0. Such a binding may also explain why the transference number of Br^- and its contribution to crystal conductivity, κ_{cr}^-, are smaller than those of Cl^-, despite the fact that the hydrated radius of Br^- is smaller than that of Cl^-.

3.5. Ionic mobilities in crystals

As can be seen in Tables 3 and 4 and in Fig. 6, the mobility of cations is 3.5–50 fold lower and that of anions is 100–300 fold lower in the tetragonal crystal as compared to the solutions, despite the fact that our calculations give an upper limit for the average mobility of intracrystalline ions.

Although anions transfer most of the current in the crystal and their contribution to the conductivity at pH 4.0 in 0.075 M NaCl is 8.5 times higher than that of cations, mobility of anions under these conditions is 40 times smaller than that of cations. As Fig. 6 illustrates, mobilities of both anions and cations in solution are mainly determined by their hydrated radius, since all data fit the same curve. In contrast, mobilities of cations and anions are completely different in crystals not only by their value but also by

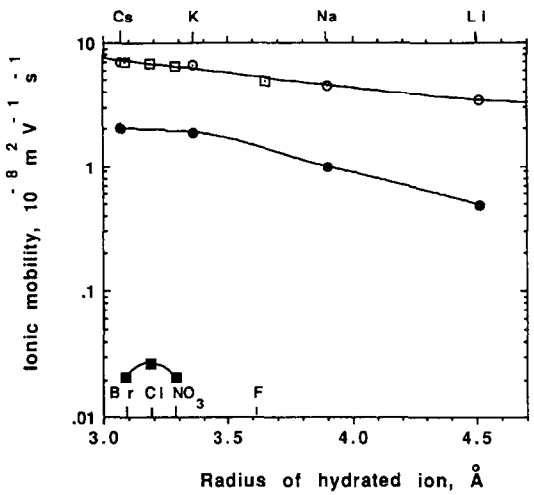

Fig. 6. Size dependence of ion mobility in dilute solutions and in the tetragonal lysozyme crystal. (○ and □) cation and anions in solution; (● and ▪) mobility of these ions in the [001] direction of the crystal equilibrated with 0.075 M salt solutions at pH 4.0 in the buffer specified in Materials and Methods. Hydrated radii of ions were taken from Ref. [20].

the mobility dependence on r_h. Whereas cation mobility drops with r_h increase both in crystals and in solutions, anions do not show this tendency. As shown in Fig. 6, the mobility of Br^- ions is less than that of Cl^-, which have a larger r_h.

The data in Table 3 show, that anions have the smallest mobility, U_{cr}^-, when the crystal is in dilute acidic solutions and when the lysozyme has the largest positive net charge. Their mobility increases with increasing pH and ionic strength, i.e., with a decrease in total number of positive charges and with an increase of their screening. On the contrary, the mobility of cations decreases as the number of negative charges on the lysozyme molecules increase with pH. The mobility of cations also decreases with an increase in salt concentration which may be explained by an increase in the retarding effect of neighboring mobile counter-ions. That is why cations have the largest mobility in dilute acidic solutions. The closer pH_{out} is to pH_{in} and to $pI = 11.2$, the less is the difference between numbers of positive and negative charges on the lysozyme molecule and the smaller is the difference between cation and anion mobilities, as seen from Table 3.

4. Discussion

4.1. Protein crystals as a new material of biotechnology

As it has been mentioned in the Introduction, cross-linked protein crystals are now coming into use as chemosensitive elements of biosensors [2,3] and as ultra stable catalysts in biotechnology [4]. The ability of protein molecules to recognize and specifically bind their ligands is exploited in both applications. Enzyme reactions in crystals and binding of specific ligands are also studied to check if proteins retain their properties upon crystallization [1]. Answering this question is very important, since most of our knowledge about protein structure has been obtained in X-ray analysis of protein crystals. However, in such studies it is not always taken into account, that not only changes in protein structure and functional mobility, but also changes in ionic composition, ligand concentration and pH inside the crystals (as compared to the external solution) may notably modify protein properties. Thus, enzymes immobilized within protein films [26] and in polyelectrolyte gels [24] show notable shifts in pH optimum of reaction and changes in Michaelis constants for charged substrates. Quantitative analysis made for polyelectrolyte gels by Katchalski et al. [24,25] has shown, that these changes are entirely determined by the electrostatic potential and potential-induced redistribution of ions between external solution and gel.

Electric properties of protein films have not been studied as quantitatively as gels. Measurements of transference numbers in glutaraldehyde cross-linked human serum albumin films, made by De Villardi et al. [21] and direct isotope measurements of concentrations of $^{24}Na^+$ and $H_2^{32}PO_4^-$ in films of bovine serum albumin and other proteins [26–28] have shown, that amorphous protein films also selectively concentrate cations or anions depending upon the sign of net charge on the protein molecule at a given pH and ionic composition of solutions. However, in contrast to gels, no quantitative analysis has been done to ensure that the Donnan potential is the only reason for ion redistribution.

Our pH titration experiments on lysozyme crystals let us quantitatively estimate and compare theoretical

and experimental concentrations of different ions in lysozyme crystals. Results of such a comparison presented above indicate that ions freely moving inside the crystals and not binding to protein molecules, like Na^+ and Cl^-, are distributed according to the electrostatic potential. In this respect protein crystals are not different from the polyelectrolyte gels. This means, that like in gels [18,24], pH optimum and Michaelis constants in crystalline enzymes should be changed as compared to solutions if the reaction is pH dependent or substrates are charged. Moreover, this shift can be quantitatively calculated from the Donnan potential, like in gels. Though seemingly trivial, such a conclusion is not so obvious because in contrast to gels the size of channels in protein crystals is comparable to that of hydrated ions and because most of the intracrystalline water (0.3 g of total 0.45 g/g protein in tetragonal lysozyme crystals) is referred to as hydrated water which possesses some physical properties different from those in bulk water (see review [29]), for example, it does not crystallize below 0°C.

4.2. Crystal channels as a model of biological channels

It has been recently demonstrated, that some specific features of biological channels, which were believed to be inventions of Mother Nature, turned out to be pure physical phenomena. Thus, the ability of biological channels to fluctuate between open and closed states, which for long time was thought to be a result of a well organized physical movement of a part of the channel structure [12], can be reproduced on a pure synthetic membrane without any protein or lipid [30] or on a patch pipette in the absence of any membrane [31]. Other typical characteristics of biological membranes, like cation selectivity, as well as inhibition by divalent cations and protons can also be reproduced on these model systems.

To obtain all these features it is enough to have a pore of 10–14 Å in diameter, or less, as it was shown in Ref. [30]. According to Wang and Imoto [32], the pore size in the acetylcholine receptor (AChR) channels is 6–7.5 Å and size is the major structure determinant of the cation permeability sequence in these channels. Such size of bottle necks is typical for channels in protein crystals, as it is illustrated in Fig. 7A and B for tetragonal and triclinic lysozyme crystals. That is why channels in protein crystals may be a good model to study physical processes in biological channels, with which they have much in common.

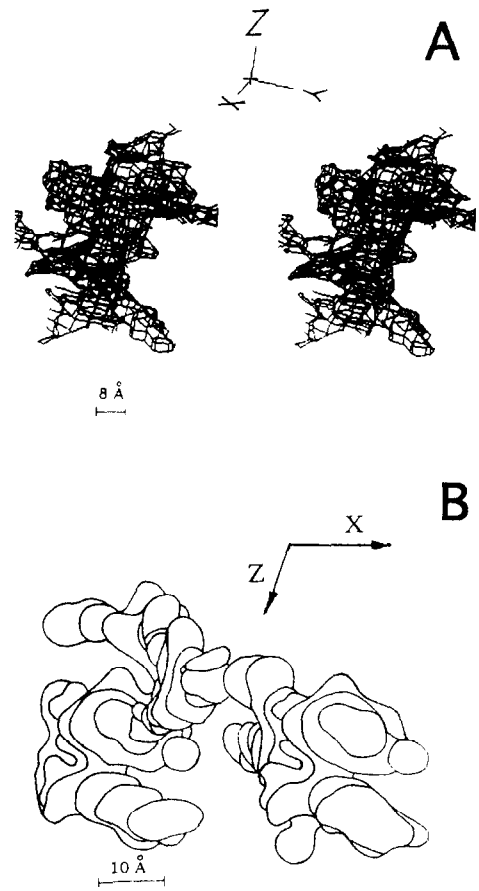

Fig. 7. View of solvent-filled channels within tetragonal (A) and triclinic (B) lysozyme crystals, according to the X-ray data. (A) Space inside the isoelectronic lines represents a stereo pair of the channel body in the tetragonal crystal. Isoelectronic lines are drawn for the electronic density intermediate between the density of protein and solvent using the CHANNEL program [33]. Electronic densities were calculated using coordinates of 6LYS taken from Brookhaven PDB. (B) Channel cross-sections parallel to the (010) crystallographic plane were drawn using the CHANNEL program and coordinates obtained in our X-ray analysis of the cross-linked triclinic crystal [34]. The distance between neighboring sections is 1.67 Å. Sections were smoothed by rolling a circle 6 Å in diameter. For better viewing of the channel each next section is shifted by 2 Å along x direction. x, y and z denote directions of crystallographic axes.

First of all, they are made from the same protein

"material". Second, their cross-sections are highly variable along the channel axes: from 30–40 Å to 6–12 Å in crystals and from 25 Å at the channel input [35] to 6–7.5 Å in the narrow part of AChR channel [32,35]. Third, they have similar conductance. Conductivity of the tetragonal crystal, κ_{cr}, measured here can be converted into the conductance of one channel, q, with a length similar to that of an AChR channel (l is about 100 Å according to Ref. [35]). Taking into account, that 1 cm^2 of the (001) plane contains $n = 2/a^2 = 3.2 \cdot 10^{12}$ channels (a is the lattice cell parameter, 2 is the number of channels per unit cell cross-section), we have $q = \kappa_{cr}/l \cdot n = 18–54$ pS in 0.1 M NaCl at 18°C and pH between 4.0 and 8.0. These estimates are in good agreement with the conductance of AChR channels with $q_{Na} = 43.2$ pS at pH 7.2 and similar other conditions [36]. Fourth, it was surprising for us to find, that both channels display similar cation selectivities, despite the fact, that the lysozyme channels have basically anionic and the AChR channels have cationic conductivity. As related to the mobility of K^+ (U_x/U_K), the cation sequence for the tetragonal crystal is: Li(0.26) < Na(0.53) < K(1.0) < Cs(1.08) and for the permeability ratios in AChR channels it is: Li(0.71) < Na(0.96) < K(1.0) < Cs(1.09) [22]. This corresponds well to the conclusion of Wang and Imoto [32], that not the charge, but the pore size determines the cation selectivity of AChR channels. Fifth, both AChR channels and those in lysozyme crystals are pH sensitive. But since the former are negatively charged they are closed with increasing H^+ concentration, whereas the latter, being charged positively, decrease their conductance with an increase in concentration of OH^-, as shown in Fig. 2.

All the above-mentioned similarities indicate, that channels in protein crystals are very good models of biological ones. What kind of new information about biological channels can we obtain when studying crystalline models? As follows from the results of this paper, the main advantage of immobilized protein crystals is a possibility to perform pH titration and to know the dependence of the net charge on the channel walls as a function of pH. This allows us to calculate the electrostatic potential and internal concentrations of ions in channels, provided that the amount of water is known. Internal concentrations can also be easily measured experimentally by isotope, X-ray fluorescence or other methods. From these concentrations, and data on conductivity and transference numbers, the mobilities of ions in channels can be calculated. And then we are able to find interesting features of ion transport in channels. For example, as shown here, anion mobility at pH 4.0 and 0.075 M NaCl is 40 times smaller than that of cations, despite the fact, that under these conditions anions transfer 8.5 times more current than cations (see Tables 1 and 3).

Another example: it has been shown recently for AChR channels, that a decrease in its net negative charge results in a decrease of the channel conductance for K^+ [37]. But from these data it is impossible to conclude whether the changes in the intrachannel K^+ concentration or in the cation mobility are responsible for that fact. We also observed a decrease in anionic conductivity in response to a decrease of the positive net charge of crystalline channels (Table 3). However, in our case, estimates of anion mobilities and concentrations clearly show, that not the mobility but the concentration decrease is responsible for the observed effect.

But the most obvious advantage of crystals as models for biological channels is the exact knowledge of atomic structure of crystalline channels. The exact position of ionizible groups from X-ray studies combined with data on their ionization states from pH titration experiments allow a precise simulation of transport within the channels. We have recently made computer simulations of diffusion of a spherical non-charged body in the channels of the tetragonal lysozyme and calculated to what extent steric limitations can reduce its mobility in the crystal as compared to that in free space [7]. Taking this ratio for bodies with a radius equal to that of hydrated ions we found their mobilities in the tetragonal crystal by multiplying the ratio with the mobility of the ions in dilute solutions [13]. These estimates, of course, account only for steric limitations for the ion motion in the crystal. Fig. 8 presents both theoretical and experimental values of cation mobilities along [001] direction plotted as a square root of mobility, $\sqrt{U^+}$, versus the radius of the hydrated ion, r_h. Such a plot is based on a simple assumption, that the flow of particles through a channel, having radius r_o, should be proportional to the part of the channel cross-section, accessible for stochastic motions, i.e.,

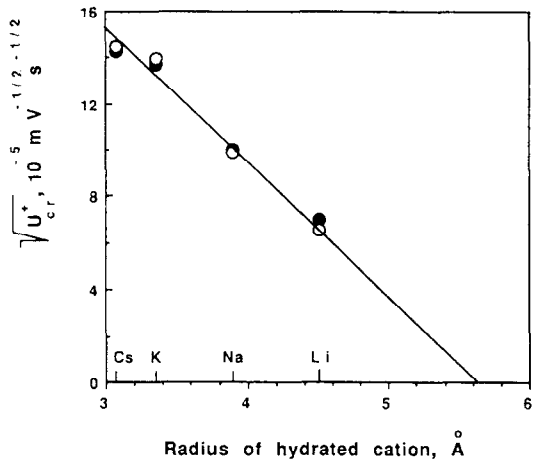

Fig. 8. Comparison of the experimental values of cation mobility in lysozyme crystals with the theoretical ones, accounting only for steric limitations to motion of hydrated ion in the crystalline channel. (○) Theoretical mobilities of ions; (●) experimental mobility measured in 0.075 M salt solutions at pH 4.0 in the buffer specified in Materials and Methods. Hydrated radii for cations are taken from Ref. [20].

to $\pi(r_o - r_h)^2$. As can be seen from Fig. 8, such a plot really reveals a linear dependence of $\sqrt{U^+}$ on r_h both for theoretical and experimental values, which well fit the same line. Extrapolation of the line in Fig. 8 to the intersection with the abscissa gives an estimate for the narrow part of the intracrystalline channel, 5.6 Å, which is in excellent agreement with computer simulations, showing termination of random walk of the probing body when its radius reaches 5.5 Å [7].

Good agreement between the theoretical and experimental data indicates that mobilities of cations in the crystal equilibrated with dilute solutions at low pH (large positive charge on lysozyme) reach maximum values available for a spherical neutral body with a diameter similar to that of hydrated ion. It is amazing, but under these conditions cations move within the highly charged channels like neutral bodies. In other words, within the channels they have the same average mobilities as in a dilute bulk solution, despite the measured average mobility in the crystal is 3.5–7 fold reduced due to steric limitations.

At all other conditions mobilities of both cations and anions in the crystal channels are considerably lower than in dilute solutions (6–11 times for cations and 70–90 times for anions), as it follows from a comparison of experimental data (Tables 3 and 4) and results of computer simulations with regard to steric limitations only [7]. Electrostatic interactions with other bound charges and free ions, specific binding of ions, changes in channel size or in properties of the intracrystalline water might be the main reasons responsible for such a discrepancy. The self-diffusion coefficient of the intracrystalline water in the tetragonal crystal is reduced by no more than 30–40% as compared to that of bulk water and it is little affected by changes in pH and in salt concentration [7]. Crystal sizes also vary only slightly (see Results). Thus, drastic changes in ion mobilities with pH and ionic strength can be caused only by changes in electrostatic interactions or in specific binding of ions when the latter exists.

5. Conclusion

Most of the conclusions in this article have been obtained from thermodynamic analysis of macroscopic characteristics averaged over the whole ensemble of crystal channels. That is why they are true until we consider the average properties of crystal or any of its part containing no less than one unit cell. They should also correctly describe selectivity sequences for ions and dependencies of their average mobilities within the channels on pH, ionic strength, etc. However, if one would like to know what factors determine these characteristics, the heterogeneity of the crystal at the level of unit cell, i.e., variations in the cross-section of the channel and irregularities in the distribution of positive and negative charges inside the channel, should be taken into consideration. In this context it is interesting to note, that the cation mobility decreases 6–7 times with an increase of pH_{in} from 5.2 to 9.6. One possible mechanism for this decrease in cation mobility may consist in increased irregularity of electric field when numbers of positive and negative charges become closer. To account for the effects of such irregularities in channel structure and electric field it is necessary to consider models and to make simulations similar to those used in analysis of biological channels. However, the advantage of crystals lies in the fact that the structure of crystal channels is known with a much higher precision and much more experimental pa-

rameters can be compared with theoretical ones to refine models and to make modeling more comprehensive and reliable.

Acknowledgements

The authors express their gratitude to Professor B. Atanasov for fruitful discussions and collaboration in performing pH titration of lysozyme crystals.

References

[1] J.A. Rupley, in S.N. Timasheff and G.D. Fasman (Editors), Structure and Stability of Biological Macromolecules, Marcel Dekker, New York, 1969, p. 291.
[2] V.N. Morozov and T.Ya. Morozova, Proc. 5th Internat. Conf. Chem. Biotechnol. Biol. Active Natural Products, Vol. 4, Varna, Bulgaria, 1989, p. 66.
[3] V.N. Morozov and T.Ya. Morozova, Anal. Biochem., 201 (1992) 68.
[4] N.L. St.Clair and M.A. Navia, J. Am. Chem. Soc., 114 (1992) 7314.
[5] B.W. Mattews, J. Mol. Biol., 33 (1968) 491.
[6] A. Shrake and J.A. Rupley, J. Mol. Biol., 79 (1973) 351.
[7] V.N. Morozov, G.S. Kachalova, V.U. Evtodienko, N.F. Lanina and T.Ya. Morozova, Eur. Biophys. J., 24 (1995) 93.
[8] L.K. Steinrauf, Acta Crystallogr., 12 (1959) 77.
[9] V.N. Morozov and T.Ya. Morozova, Biopolymers, 20 (1981) 451.
[10] P.J. Robinson, P. Dunhill and H.D. Lilly, Biochim. Biophys. Acta, 242 (1971) 659.
[11] B.A. Lopatin, Conductometry (Measurements of Conductivity of Electrolytes), Nauka, Novosibirsk, 1969.
[12] B. Hill, Ionic Channels of Excitable Membranes, Sinauer, Sunderland, MA, 1992, p. 186.
[13] J.A. Dean, Lange's Handbook of Chemistry, 40th ed., McGraw-Hill, New York, 1992.
[14] S.S. Dukhin, Electroconductivity and Electrokinetic Properties of Dispersed Systems, Naukova Dumka, Kiev, 1975, p. 209.
[15] Yu.Yu. Lurje, Handbook of Analytical Chemistry, Chimia, Moscow, 1967, p. 104.
[16] B.R. Nikolskii (Editor), Chemist's Handbook, Vol. 3, Chimia, Moscow, Leningrad, 1965, p. 591.
[17] C. Tanford and R. Roxby, Biochemistry, 11 (1972) 2192.
[18] L. Goldstein, Methods Enzymol., 44 (1976) 401.
[19] V.N. Morozov, T.Ya. Morozova, G.S. Kachalova and E.T. Myachin, Int. J. Biol. Macromol., 10 (1988) 329.
[20] J. Cêleda, Collect. Czech. Chem. Commun., 53 (1988) 433.
[21] M. de Villardi, M. Delmotte and A. Rejou-Michel, Bioelectrochem. Bioenergetics, 12 (1984) 517.
[22] T. Konno, Ch. Busch, E. Von Kitzing, K. Imoto, F. Wang, J. Nakai, M. Mishina, Sh. Numa and B. Sakmann, Proc. R. Soc. London, B244 (1991) 69.
[23] K.J. Palmer, M. Ballantyne and J.A. Galvin, J. Am. Chem. Soc., 70 (1948) 906.
[24] L. Goldstein, Y. Levin and E. Katchalski, Biochemistry, 3 (1964) 1913.
[25] A. Katchalski, in J.A.V. Butler and J.T. Randall (Editors), Progress in Biophys. Biophys. Chem., Vol. 4, Pergamon, London, 1954, p. 1.
[26] A. Friboulet and D. Thomas, Biophys. Chem., 16 (1982) 145.
[27] A. Friboulet and D. Thomas, Biophys. Chem., 16 (1982) 139.
[28] J.N. Barbotin, A. Friboulet, Y. Malpiece and D. Thomas, Colloids Surf., 10 (1984) 359.
[29] J.A. Rupley and G. Carreri, Adv. Prot. Chem., 41 (1991) 37.
[30] A.A. Lev, Y.E. Korchev, T.K. Rostovtseva, C.L. Bashford, D.T. Edmonds and C.A. Pasternak, Proc. R. Soc. London, B252 (1993) 187.
[31] F. Sachs and F. Qin, Biophys. J., 65 (1993) 1101.
[32] F. Wang and K. Imoto, Proc. R. Soc. London, B250 (1992) 11.
[33] O.P. Kisluk, G.S. Kachalova and N.F. Lanina, J. Mol. Graphics, 12 (1994) 305.
[34] G.S. Kachalova, V.N. Morozov, T.Ya. Morozova, E.T. Myachin, A. Vagin, B.V. Strokopytov and Yu. V. Nekrasov, FEBS Lett., 284 (1991) 91.
[35] C. Toyoshima and N. Unwin, Nature, 336 (1988) 247.
[36] A. Villarroel, S. Herlitze, M. Koenen and B. Sakmann, Proc. R. Soc. London, B243 (1991) 69.
[37] K. Imoto, C. Busch, B. Sakmann, M. Mishina, T. Konno, J. Nakai, H. Bujo, Y. Mori, K. Fukuda and S. Numa, Nature, 335 (1988) 645.